Table 3.1 Experimental, Low Speed NACA Airfoil Data for Smooth Leading Edges

(Note: Data reproduced from Reference 3.1 for $R_N = 9 \times 10^6$)

Airfoil	α_0 (deg)	$\bar{c}_{m_0}$	c_{l_α} (1/deg)	$\bar{x}_{ac}$	$\alpha_{c_{l_{max}}}$ (deg)	$c_{l_{max}}$	α^* (deg)
0006	0	0	0.108	0.250	9.0	0.92	9.0
0009	0	0	0.109	0.250	13.4	1.32	11.4
1408	–0.8	–0.023	0.109	0.250	14.0	1.35	10.0
1410	–1.0	–0.020	0.108	0.247	14.3	1.50	11.0
1412	–1.1	–0.025	0.108	0.252	15.2	1.58	12.0
2412	–2.0	–0.047	0.105	0.247	16.8	1.68	9.5
2415	–2.0	–0.049	0.106	0.246	16.4	1.63	10.0
2418	–2.3	–0.050	0.103	0.241	14.0	1.47	10.0
2421	–1.8	–0.040	0.103	0.241	16.0	1.47	8.0
2424	–1.8	–0.040	0.098	0.231	16.0	1.29	8.4
23012	–1.4	–0.014	0.107	0.247	18.0	1.79	12.0
23015	–1.0	–0.007	0.107	0.243	18.0	1.72	10.0
23018	–1.2	–0.005	0.104	0.243	16.0	1.60	11.8
23021	–1.2	0	0.103	0.238	15.0	1.50	10.3
23024	–0.8	0	0.097	0.231	15.0	1.40	9.7
64–006	0	0	0.109	0.256	9.0	0.80	7.2
64–009	0	0	0.110	0.262	11.0	1.17	10.0
64_1–012	0	0	0.111	0.262	14.5	1.45	11.0
64_1–212	–1.3	–0.027	0.113	0.262	15.0	1.55	11.0
64_1–412	–2.6	–0.065	0.112	0.267	15.0	1.67	8.0
64–206	–1.0	–0.040	0.110	0.253	12.0	1.03	8.0
64–209	–1.5	–0.040	0.107	0.261	13.0	1.40	8.9
64–210	–1.6	–0.040	0.110	0.258	14.0	1.45	10.8
64A010	0	0	0.110	0.253	12.0	1.23	10.0
64A210	–1.5	–0.040	0.105	0.251	13.0	1.44	10.0
64A410	–3.0	–0.080	0.100	0.254	15.0	1.61	10.0
64_1A212	–2.0	–0.040	0.100	0.252	14.0	1.54	11.0
64_2A215	–2.0	–0.040	0.095	0.252	15.0	1.50	12.0

Note: For definition of symbols, see the list of Symbols

3.3.3 PITCHING MOMENT CURVE: c_m VERSUS c_l or c_m VERSUS α

Figure 3.5a shows typical airfoil data for c_m versus c_l and c_m versus α .

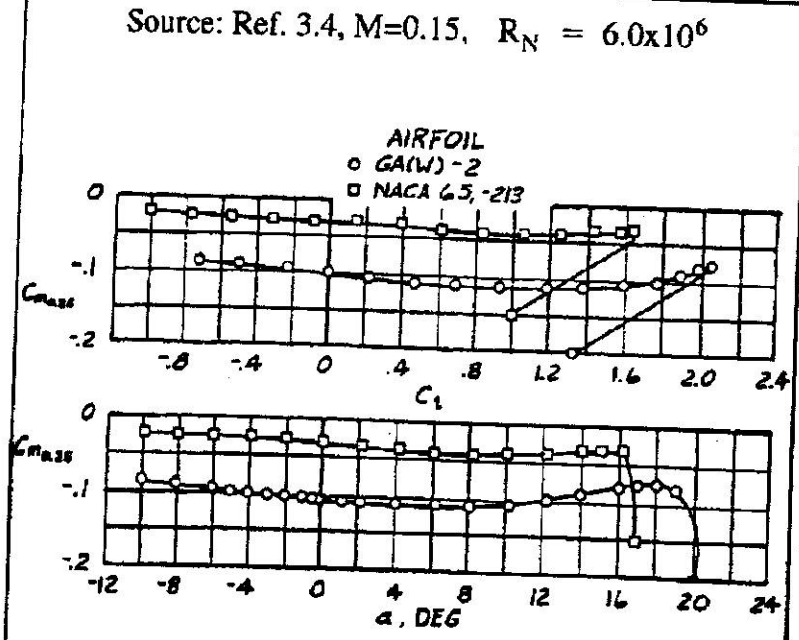

Figure 3.5a Pitching Moment Coefficient Plots for Two Airfoils

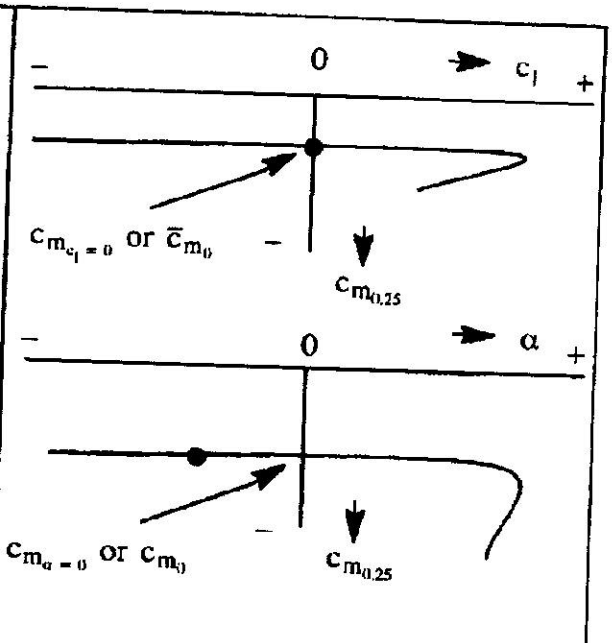

Figure 3.5b Generic Plots of Pitching Moment Coefficient Versus Lift Coefficient and Versus Angle of Attack

The magnitude of the pitching moment coefficient, c_m depends on the location of the moment reference center. This moment reference center is normally identified in a subscript to c_m .

In Figure 3.5a the moment reference center is the quarter chord point, identified in the subscript as 0.25c or simply 0.25. Generic plots of c_m versus c_l and c_m versus α are shown in Figure 3.5b. Numerical values for the parameter c_{m_0} are given in Table 3.1 for several types of airfoil.

A very important reference point on an airfoil is its so–called aerodynamic center or a.c. The aerodynamic center is defined as that point about which the variation of the pitching moment coefficient with angle of attack is zero. To find the a.c., assume that in some experimental set–up the moment reference center was selected to be a distance x from the leading edge. Figure 3.6 shows the corresponding geometry. Neglecting the moment contribution due to drag it is seen that:

$$c_{m_{ac}}\bar{q}c^2 = c_{m_x}\bar{q}c^2 + c_l\bar{q}c(x_{ac} - x) \qquad (3.19)$$

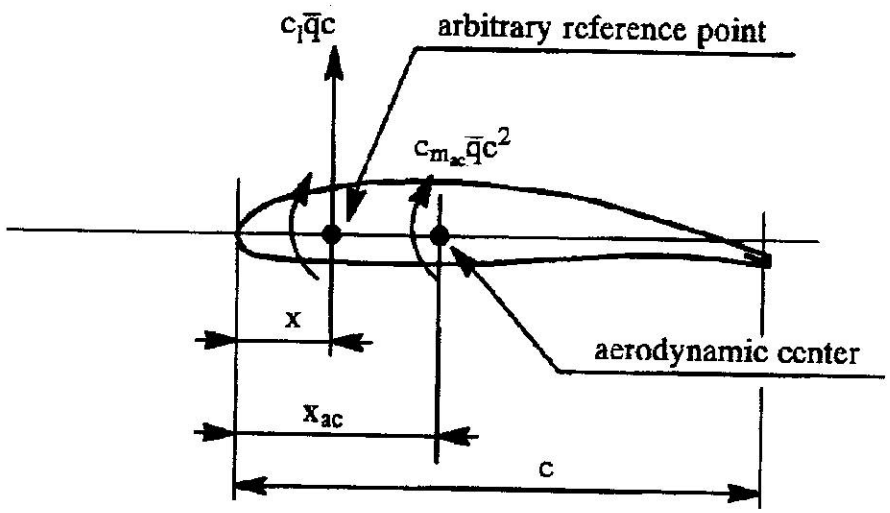

Figure 3.6 Geometry for Finding the Aerodynamic Center

$$c_{m_{ac}} = c_{m_x} + c_l\left(\frac{x_{ac} - x}{c}\right) \tag{3.20}$$

By definition, $c_{m_{ac}}$ is independent of the angle of attack, α, and therefore:

$$\frac{\partial c_{m_{ac}}}{\partial \alpha} = 0 = \frac{\partial c_{m_x}}{\partial \alpha} + \frac{\partial c_l}{\partial \alpha}\left(\frac{x_{ac} - x}{c}\right) \tag{3.21}$$

From this it follows that:

$$\frac{x_{ac}}{c} = \frac{x}{c} - \frac{\partial c_{m_x}}{\partial c_l} \tag{3.22}$$

Using experimental data of c_{m_x} versus c_l it is therefore possible to compute the location of the aerodynamic center, x_{ac} . From experimental data taken at low subsonic Mach numbers it is normally found that the aerodynamic center is at the quarter chord point: $\frac{x_{ac}}{c} \approx 0.25$.

3.4 AIRFOIL PRESSURE DISTRIBUTION

The pressure distribution over an airfoil is important for load calculations and for control surface hinge moment calculations. The pressure distribution is normally expressed in terms of the so-called pressure coefficient, c_p , which is defined as:

$$c_p = \frac{p - p_\infty}{\bar{q}_\infty} \tag{3.23}$$

$$c_{d_{min}}(\text{full scale}) = c_{d_{min}}(\text{model}) - \Delta c_{d_{min}} \tag{3.40}$$

where:

$$\Delta c_{d_{min}} = 2(\text{S.F.})[c_f(\text{model}) - c_f(\text{full scale})] \tag{3.41}$$

There still do not exist accurate theoretical methods for correcting the maximum lift coefficient from tunnel data to full scale. Jacobs and Sherman have shown some experimental results for the Reynolds number effect on $c_{l_{max}}$ for several NACA airfoils (Ref. 3.8). Additional data can be found in Ref. 3.9. Most aircraft manufacturers have their own in–house correction procedures for extrapolating tunnel $c_{l_{max}}$ data to full scale. Such procedures are then based upon their experience obtained in comparing model and airplane data.

3.7 DESIGN OF AIRFOILS

Because lifting surfaces (such as wings, tails, canards and pylons) can be thought of as spanwise arrangements of airfoils, the basic characteristics of airfoils have a major effect on the behavior of lifting surfaces. It is therefore important to be aware of those airfoil characteristics which have the potential of being 'driving' factors in airplane lift, drag, and pitching moment.

To design an airfoil for any specific requirement involving lift, drag or pitching moment, several effects of airfoil geometry on airfoil aerodynamics should be understood. It has been found that the most important geometric parameters are:

1) maximum thickness ratio, $(t/c)_{max}$
2) shape of the mean line (also referred to as camber). If the mean line is a straight line, the airfoil is said to be symmetrical.
3) leading edge shape or Δy parameter and leading edge radius (l.e.r.)
4) trailing edge angle, ϕ_{TE}

Figure 3.15 provides a geometric interpretation for these parameters, most of which were also defined in Figure 3.1. The reader should consult Ref. 3.1 for a detailed discussion of airfoil parameters and airfoil characteristics. Ref. 3.1 also contains a large body of experimental data on a variety of NACA airfoils (NACA = National Advisory Committee on Aeronautics, predecessor of NASA, the National Acronautics and Space Administration). In addition, this reference contains explanations for the numerical designations used with all NACA airfoils. Table 3.2 defines the most important NACA airfoil designations.

It is noted that the NACA 6–series airfoils were designed to have mean camber lines which produce a near uniform chordwise loading from the leading edge to a point x/c = a, and a linearly decreasing load from this point to the trailing edge. Any time this condition is met, the corresponding a–value is given after the airfoil designation.

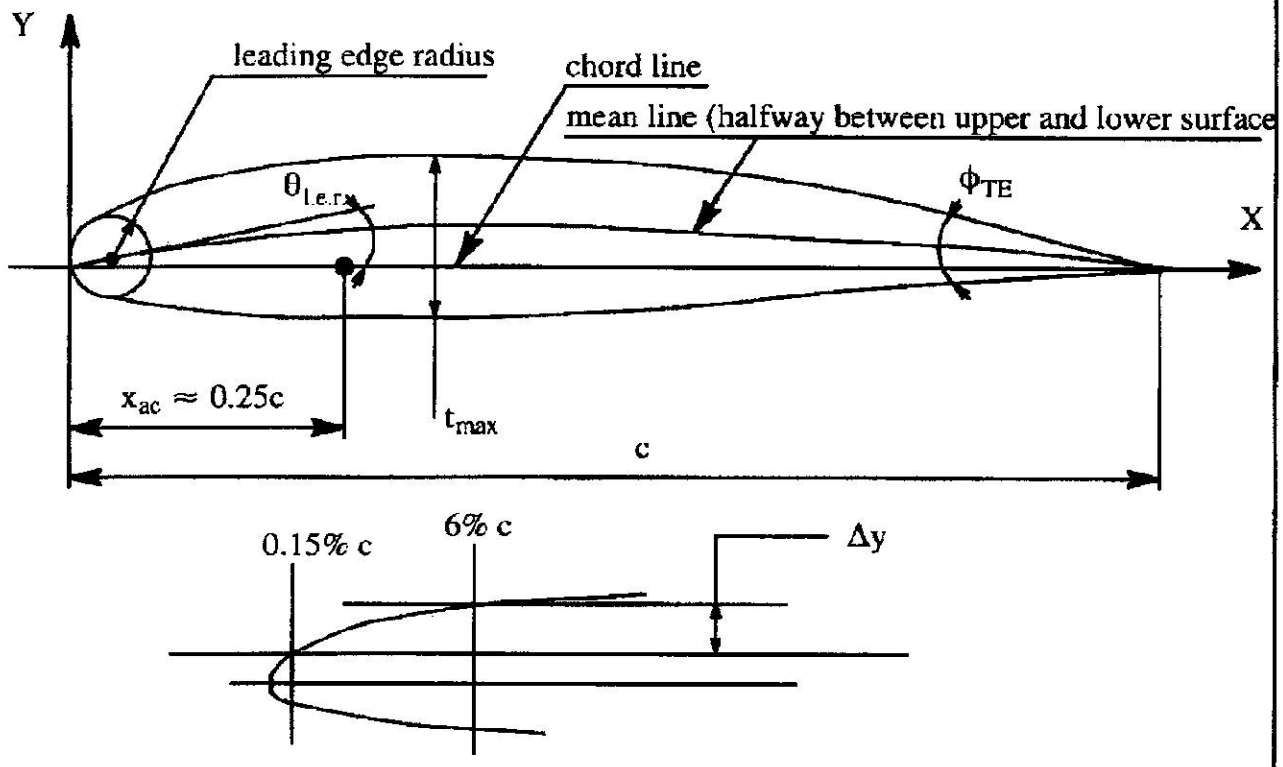

Figure 3.15 Definition of Important Airfoil Geometric Parameters

Examples are: NACA 66(215)–216 with a = 0.6 and NACA 65(318)–217 with a = 0.5. These two examples represent airfoils with thickness distributions obtained by linearly increasing or decreasing the ordinates of the originally derived distribution. In the last example, the airfoil has a 17% thickness ratio. Its ordinates were derived from the airfoil with 18% thickness distribution. The digit 3 represents in tenths, one half of the extent of the low drag range. When this digit is omitted, it implies that the low drag range is less than 0.1.

Since the late 1950's NASA has engaged in the design of airfoils for transonic transport and fighter applications. These so–called supercritical airfoils have a higher M_{dd} value than the conventional NACA 6–series airfoils as illustrated in Figure 3.13. These supercritical airfoils are characterized by very little camber in the forward portion. On the other hand, the rearward portion is severely cambered. Figure 3.16 presents an example of a supercritical airfoil.

During the course of these recent airfoil research activities, new airfoils for lower speed applications have also been derived. Examples are the low–speed airfoils, such as LS(1)–0417 and LS(1)–0413, the medium speed airfoils, such as MS(1)–0313 and natural laminar flow airfoils, such as NLF(1)–416. The LS(1)–0417 airfoil is also known as the GA(W)–1 airfoil (W stands for Whitcomb) and the LS(1)–0413 airfoil is also known as the GA(W)–2 airfoil. Figure 3.17 shows a comparison of older NACA airfoils with the GA(W)–2 airfoil. Figure 3.17 also shows a comparison of the camber and thickness distributions for the GA(W)–1 airfoil with those for the NACA 65_3–018 airfoil. Several key design features of the 17% thick GA(W)–1 airfoil are:

Table 3.2 Examples of NACA Airfoil Designations

4-digit airfoils **Example: NACA 4412**

4	camber: 0.04c
4	position of the camber at 0.4c from the leading edge (L.E.)
12	maximum thickness: 0.12c

5-digit airfoils **Example: NACA 23015**

2	camber: 0.02c
	the design lift coefficient is 0.15 times the first digit for this series
30	position of the camber at (0.30/2) = 0.15c from the leading edge (L.E.)
15	maximum thickness: 0.15c

6-series airfoils **Example: NACA 65_3-421**

6	series designation
5	minimum pressure occurs at 0.5c
3	the drag coefficient is near its minimum value over a range of lift coefficients of 0.3 above and below the design lift coefficient
4	design lift coefficient is 0.4
21	maximum thickness: 0.21c

7-series airfoils **Example: NACA 747A315**

7	series designation
4	favorable pressure gradient on the upper surface from the L.E. to 0.4c at the design lift coefficient
7	favorable pressure gradient on the lower surface from the L.E. to 0.7c at the design lift coefficient
A	a serial letter to distinguish different sections having the same numerical designation but different mean line or different thickness distribution
3	design lift coefficient is 0.3
15	maximum thickness: 0.15c

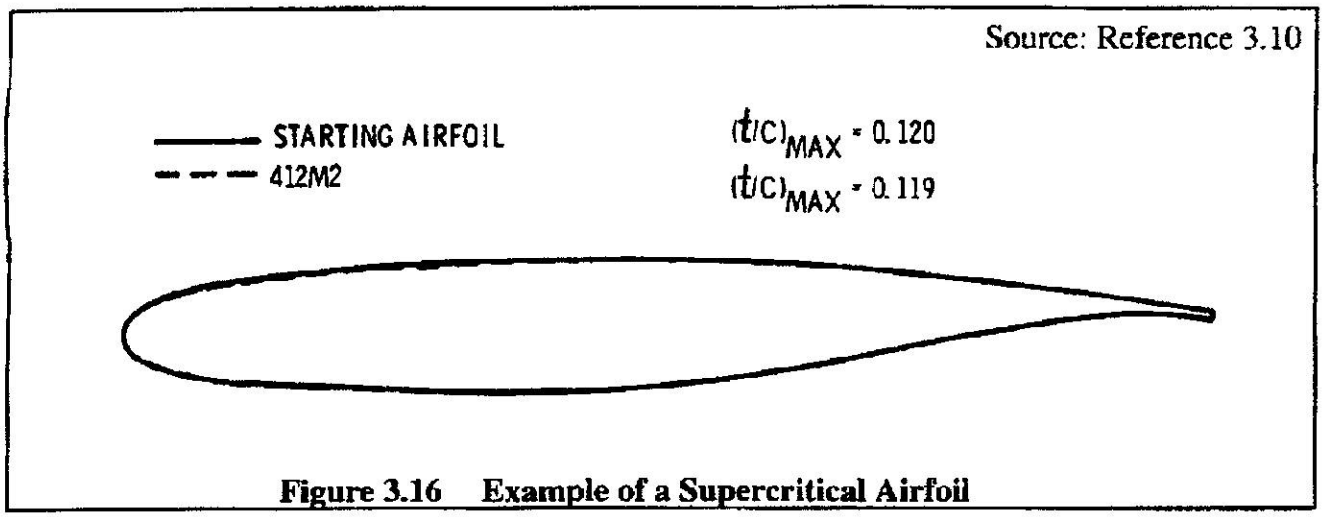

Figure 3.16 Example of a Supercritical Airfoil

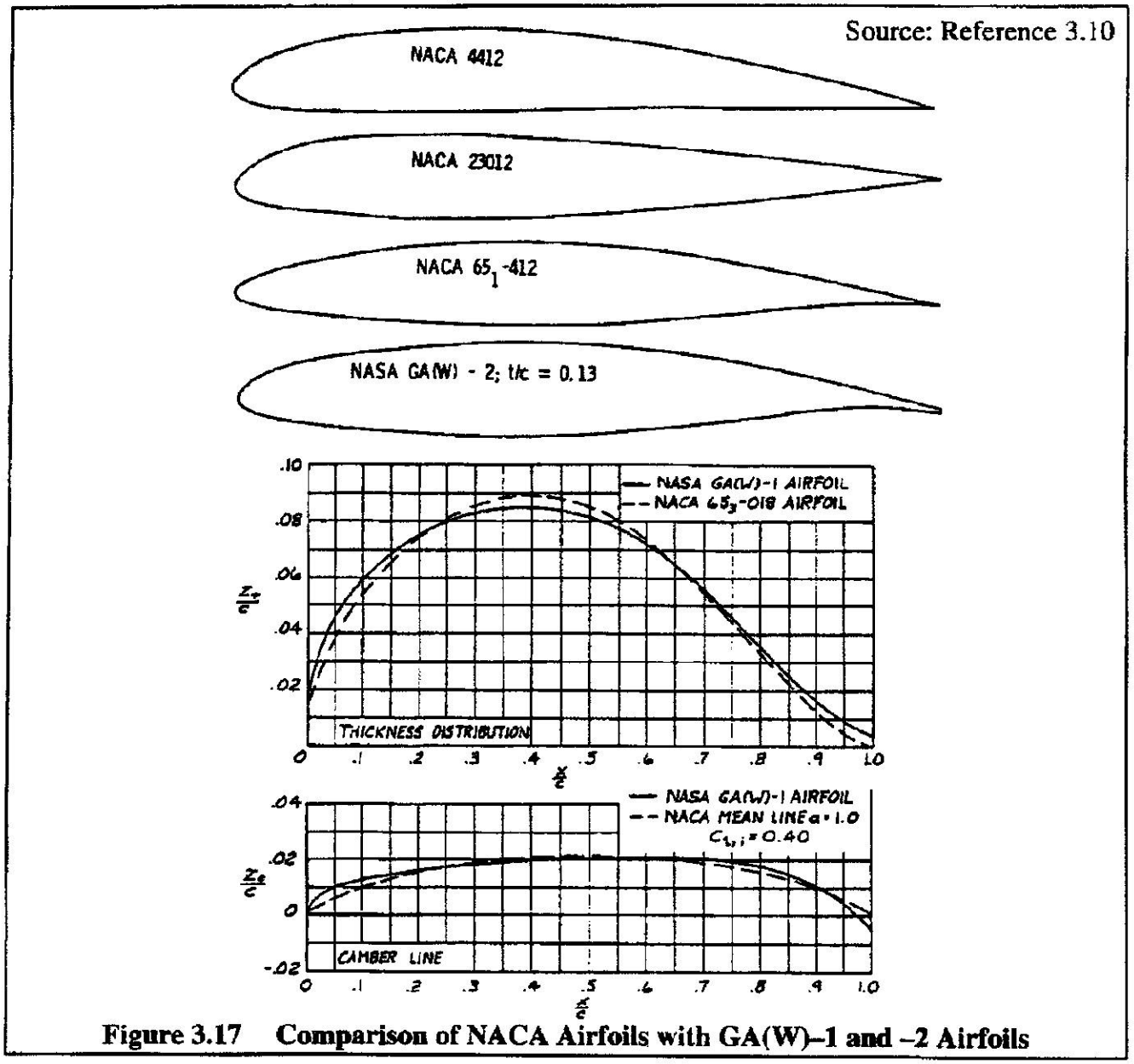

Figure 3.17 Comparison of NACA Airfoils with GA(W)–1 and –2 Airfoils

a) A large upper surface leading edge radius (0.06c) was used to alleviate the peak negative pressure coefficients and therefore delay airfoil stall to a higher angle of attack.

b) The airfoil was contoured to provide an approximate uniform chordwise load distribution near the design lift coefficient of 0.4.

c) A blunt trailing edge was provided with the upper and lower surface slopes approximately equal to moderate the upper surface pressure recovery and thus postpone the stall.

Test results in References 3.11 (for GA(W)-1) and 3.4 (for GA(W)-2) show that the section maximum lift coefficient, $c_{l_{max}}$ of this type airfoils is about 30% greater than that of a typical older NACA 6-series airfoil. This is achieved with a section lift-to-drag ratio, c_l/c_d at $c_l = 0.9$ which is about 50% greater! Figures 3.18a and 3.18b show some example data. In Figure 3.18b, the so-called NACA standard roughness is a large wrap-around roughness as compared with the narrow strip roughness strip now used as the NASA standard.

In selecting an airfoil for an airplane lifting surface (wing, canard, horizontal or vertical tail) the following considerations are important:

1) Drag (for example, one may wish to obtain the highest possible cruise speed)

2) Lift-to-drag ratio at values of the lift coefficient which are important to the airplane (for example, one may wish to design for a given climb rate with one engine inoperative)

3) Thickness (for example, one may wish to design the wing for a low structural weight)

4) Thickness distribution (for example, one may wish to design for a large internal fuel volume)

5) Stall characteristics (for example, one may wish to design for gentle stall characteristics)

6) Drag rise behavior (for example, one may wish to design for a high drag divergence Mach number. This item is closely linked to item 1).

7) Pitching moment characteristics (effect on trim drag)

It is clear from these seven items that airfoil design and/or airfoil selection will have to be done with a number of compromises in mind to achieve an acceptable overall result. Table 3.3 lists a number of practical airfoil applications.

Part VI of Reference 3.10 may be consulted for rapid, empirical methods to predict section lift, drag and pitching moment characteristics from the basic geometric parameters seen in Figure 3.14.

Source: Reference 3.10

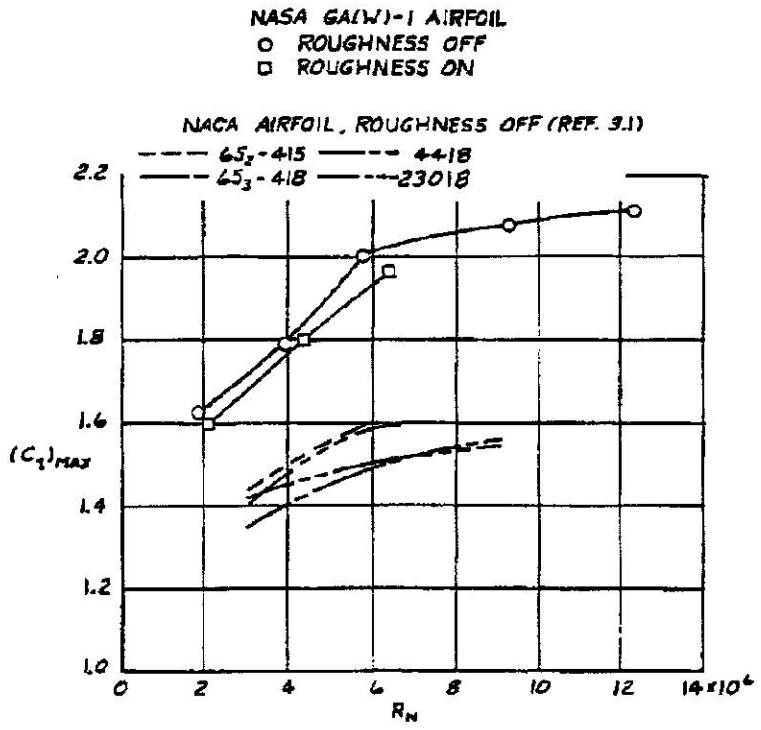

M = 0.15

a) Variation of Section Maximum Lift Coefficient with Reynolds Number

Source: Reference 3.10

$R_N = 6 \times 10^6$ and M = 0.2

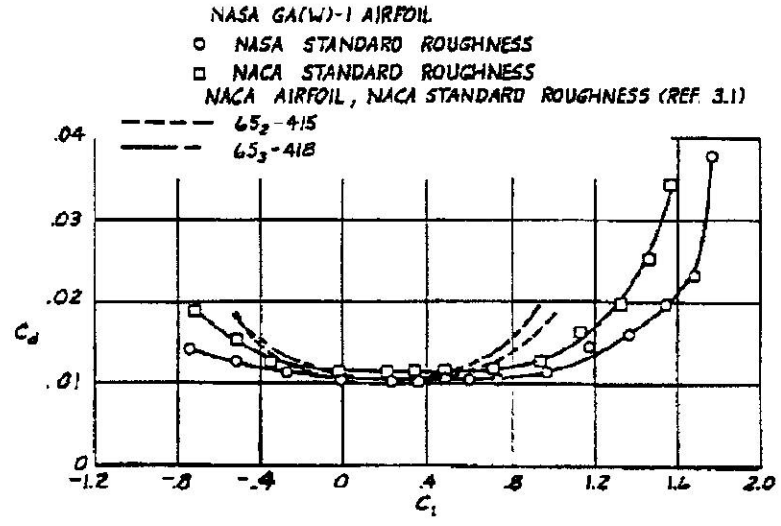

b) Variation of Section Drag Coefficient with Section Lift Coefficient

Figure 3.18 Comparison of Aerodynamic Characteristics of Some NACA and NASA Airfoils

Table 3.3 Examples of Airfoil Applications

Airplane Type	Wing	Horiz. Tail	Vert. Tail
Beech Bonanza	NACA 23016.5 (mod) at root NACA 23012 (mod) at tip –3° twist	NACA 0009	NACA 0009
Beech Queen Air B80	NACA 23020 (mod) at root NACA 23012 (mod) at tip –3° 54' twist	NACA 0009	NACA 0009
Beech Skipper	NASA GA(W)–1	NACA 0009	NACA 0009
Beech Duchess	NACA 63_2A415 (mod) at root	NACA 0009	NACA 0009
Cessna 210 Centurion	NACA 64_2A215 at root NACA 64_1A412 at tip –2° twist	NACA 0009	NACA 0009
Cessna T–37	NACA 2418 at root NACA 2412 at tip	NACA 0012	NACA 0012
Cessna 337 Skymaster	NACA 2412 at root NACA 2409 at tip –2° twist	NACA 0009	NACA 0009
Cessna 500 Citation	NACA 23014 (mod) at root NACA 23012 at tip –3° twist	NACA 0009	NACA 0009
Piper PA–23 Aztec	USA*35–B (mod) t/c = 14% –2.5° twist	NACA 0009	NACA 0009
Piper PA–31T Cheyenne	NACA $63_2$415 at root NACA 63 A212 at tip –2.5° twist	NACA 0009	NACA 0009
Lockheed 1329–25 Jetstar	NACA 63A112 at root NACA 63A309 at tip –2° twist	NACA 0009	NACA 0009
LTV A–7 Corsair	NACA 65A007	Not available	Not available
Northrop F–5A	NACA 65A004.8 (mod)	Not available	Not available
Boeing 747	Boeing proprietary airfoils. t/c=13.44% inboard t/c=7.8% mid–span t/c=8% tip	Not available	Not available

3.8 AIRFOIL MAXIMUM LIFT CHARACTERISTICS

The maximum lift characteristics of an airfoil as well as the associated stall behavior are of great importance to airplane performance.

Whenever the airflow around an airfoil separates, stall is said to have started. From a $c_l - \alpha$ viewpoint there are two types of stall: gradual and abrupt. Figure 3.19 shows examples of each type.

Source: Reference 3.10

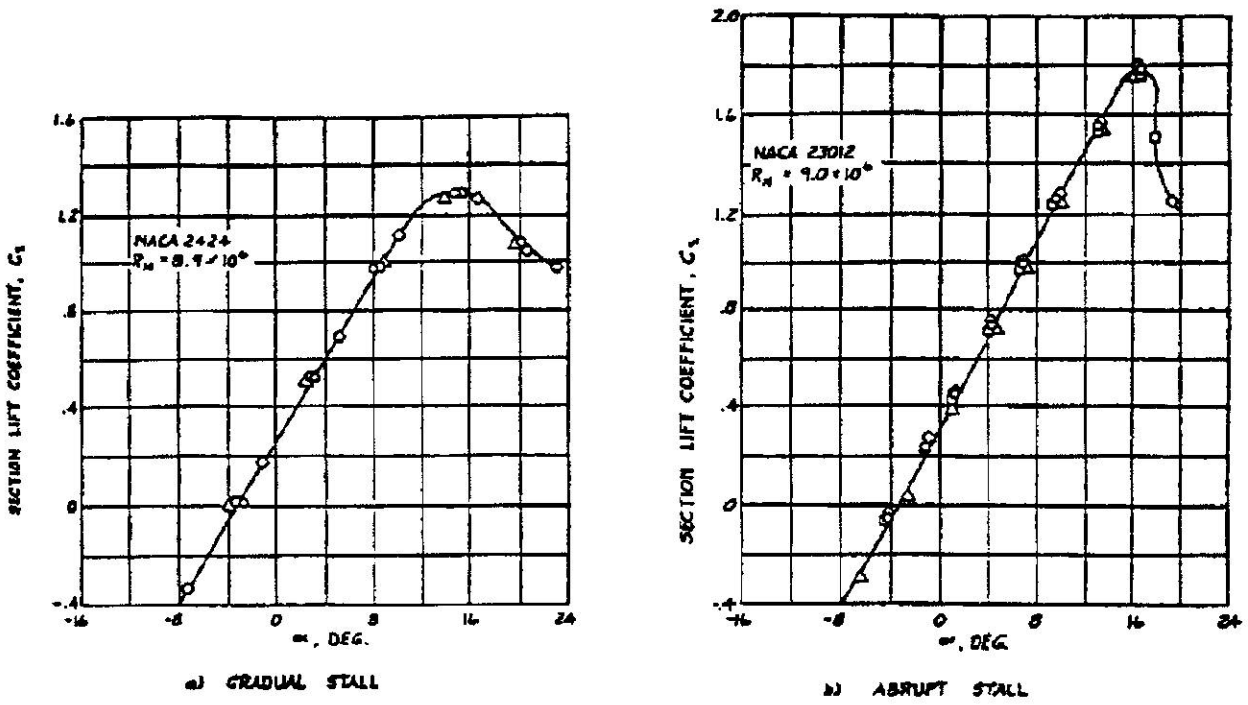

Figure 3.19 Example of Gradual and Abrupt Airfoil Stalls

The first type of stall is characterized by a gradual stall followed by a shallow drop–off of the section lift coefficient. This type of stall frequently occurs on airfoils with moderate or thick sections.

The second type of stall is characterized by an abrupt drop–off of the section lift coefficient. It is often associated with thin airfoil sections.

The main airfoil design features which affect section stall and therefore the maximum lift coefficient are:

a) thickness ratio
b) leading edge radius
c) camber
d) location of maximum thickness

These four factors are discussed in Sub–section 3.8.1.

3.8.1 GEOMETRIC FACTORS AFFECTING AIRFOIL MAXIMUM LIFT AT LOW SPEEDS

3.8.1.1 Thickness Ratio

Figure 3.20 shows how airfoil $c_{l_{max}}$ is affected by airfoil thickness ratio, t/c. It is shown in Sub–sub–section 3.8.1.2, that for a given thickness ratio, $c_{l_{max}}$ depends strongly on the leading edge radius and on the leading edge shape. Figure 3.20 also shows that the modern LS series of airfoils have considerably higher values of $c_{l_{max}}$ than conventional NACA airfoils. For the NACA airfoils, a thickness ratio of around 13% will generally produce the highest possible section lift coefficient. For the LS series of airfoils the highest vale of $c_{l_{max}}$ occurs at a thickness ratio of about 15%.

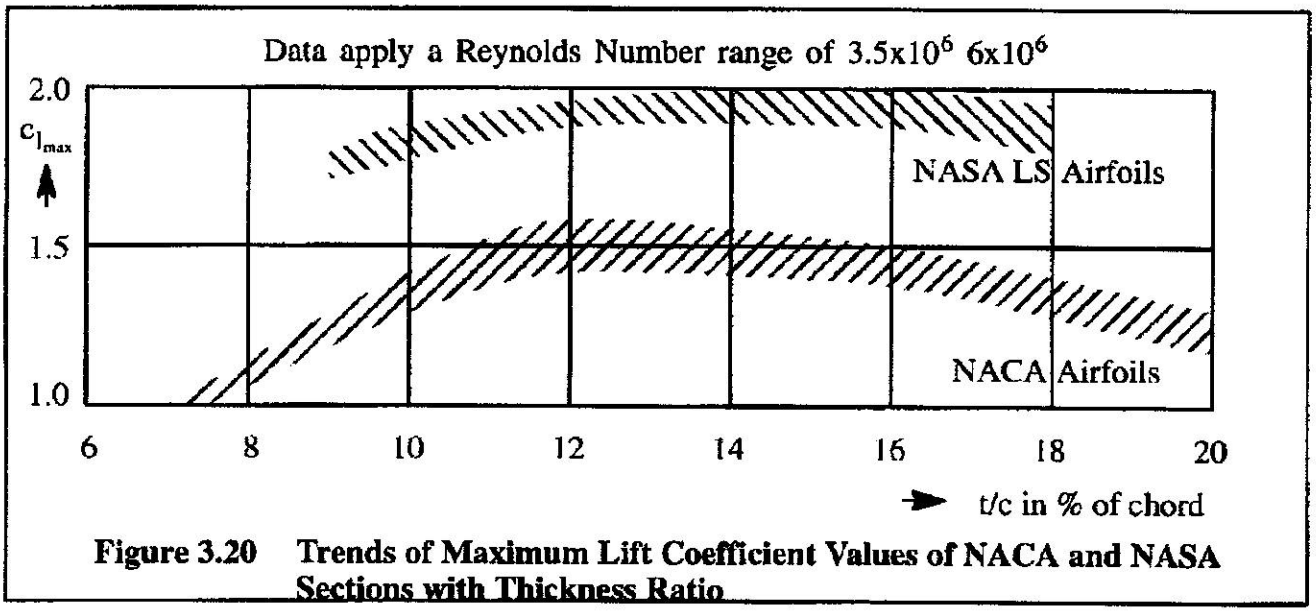

Figure 3.20 Trends of Maximum Lift Coefficient Values of NACA and NASA Sections with Thickness Ratio

3.8.1.2 Leading Edge Radius and Leading Edge Shape

The effect of leading edge radius and leading edge shape is more or less reflected in a geometric parameter, called: $\frac{z_5}{t}$, where z_5 is the local thickness of the airfoil at 5% chord and t is the maximum thickness of the airfoil. Figure 3.21 shows the effect of $\frac{z_5}{t}$ on section $c_{l_{max}}$ for NACA symmetrical airfoils of different thickness ratios. A large value of $\frac{z_5}{t}$ indicates a large leading edge radius. It is seen that large leading edge radii are beneficial in producing large values of $c_{l_{max}}$ at low speeds.

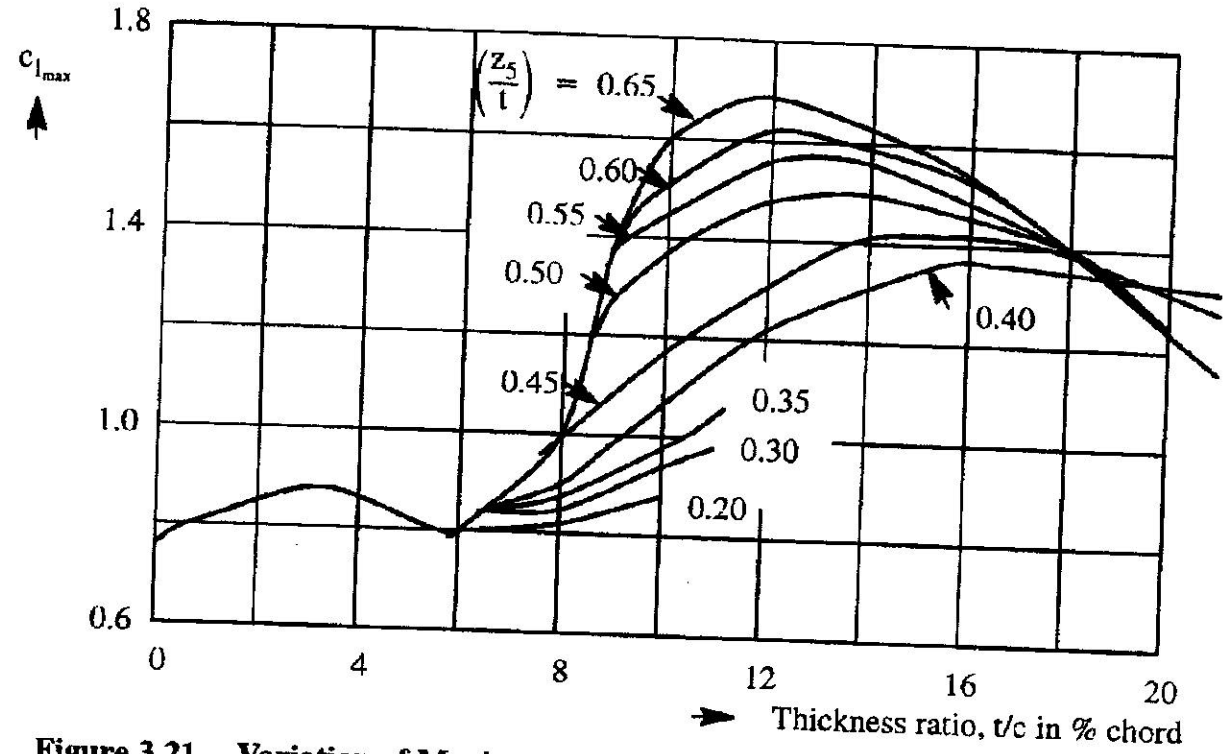

Figure 3.21 Variation of Maximum Lift Coefficient with Geometry of NACA Symmetrical Airfoils at a Reynolds Number of 6x10⁶

3.8.1.3 Camber and Location of Maximum Thickness

Experimental data show that the maximum lift coefficient of a cambered section depends not only on the amount of camber and camber line shape, but also on the thickness and nose radius of the section on which it is used.

In general, the addition of camber is always beneficial to $c_{l_{max}}$ and the benefit grows with increasing camber. The increment to maximum lift due to camber is least for sections with relatively large leading edge radii (i.e. the benefit of camber grows with reduction of the parameter $\frac{z_5}{t}$; and camber is more effective on thin sections than on thick sections.

In addition, a forward position of maximum camber produces higher values of $c_{l_{max}}$. For example, the NACA 23012 airfoil (with 2% maximum camber at 0.15 chord) has a $c_{l_{max}}$ of 1.79 as compared with 1.67 for NACA 4412 (with 4% camber at 0.4 chord but the same thickness distribution) at a Reynolds number of 9x106.